(4) Luňák, S.; Vladyka, J.; Dušek, K. *Polymer* **1978**, *19*, 931.
(5) Kamon, T.; Saito, K. *Kobunshi Ronbunshu* **1984**, *41*, 293.
(6) Dušek, K.; Illavský, M.; Luňák, S. *J. Polym. Sci., Polym. Symp.* **1976**, *53*, 29.
(7) Luňák, S.; Dušek, K. *J. Polyum. Sci., Polym. Symp.* **1976**, *53*, 45.
(8) Dušek, K. *Adv. Polym. Sci.* **1986**, *78*, 1.
(9) Gulino, D.; Galy, J.; Pascault, J. P.; Tighzert, L.; Pham, Q. T. *Makromol. Chem.* **1983**, *184*, 411.
(10) Sabra, A.; Lam, T. M.; Pascault, J. P.; Grenier-Loustalot, M. F.; Grenier, P. *Polymer* **1987**, *28*, 1030.
(11) Riccardi, C. C.; Adabbo, H. E.; Williams, R. J. J. *J. Appl. Polym. Sci.* **1984**, *29*, 2481.
(12) Riccardi, C. C.; Williams, R. J. J. *Polymer* **1986**, *27*, 913.
(13) Miller, D. R.; Macosko, C. W. *Macromolecules* **1980**, *13*, 1063.

Registry No. DER 332, 25085-99-8; PGE, 122-60-1; Laromin C 260, 6864-37-5.

Dissociation Behavior of Poly(fumaric acid) and Poly(maleic acid). 2. Model Calculation

Seigou Kawaguchi,* Toshiaki Kitano,† and Koichi Ito

Department of Materials Science, Toyohashi University of Technology, Tempaku-cho, Toyohashi 440, Japan

Akira Minakata

Department of Physics, Hamamatsu University School of Medicine, Handa-cho, Hamamatsu 431-31, Japan. *Received February 7, 1989; Revised Manuscript Received June 6, 1989*

ABSTRACT: The model calculation for the dissociation behavior of poly(fumaric acid) and poly(maleic acid) reported in the previous paper was carried out using the Ising model. The interaction between a proton and ionized groups was divided into short-range and long-range electrostatic interactions, the former being evaluated from the ratio of the activity of an ionized group to that of an unionized one and the latter from the contribution of the interaction between pairs of the ionized groups not counted in the former. The factors examined here which may affect the Gibbs free energy change in the dissociation process are the range of the short-range interaction, the configuration of ionized groups, the dielectric constant around ionized groups, and the possibility of hydrogen bonding between neighboring carboxyl groups. Agreement of the model calculation with experimental data was not as quantitative as that for the alternating copolymer of maleic acid reported previously, probably because of overestimation of the long-range interaction assuming the Debye–Hückel potential. The difference in the potentiometric titration behavior between poly(fumaric acid) and poly(maleic acid) could be explained qualitatively by their configurational difference. The strong short-range electrostatic interaction proves to play a dominant role in the dissociation behavior of these polyacids with high charge densities.

Introduction

The solution properties characteristic of polyelectrolytes are well-known to result from the electrostatic interaction either between ionized groups on a polyelectrolyte chain or between an ionized group and the surrounding low molecular weight ions in the solution. So far various kinds of models have been proposed to interpret the dissociation process of the weak poly(carboxylic acid) in terms of the electrostatic interaction between a proton and the charges of the ionized groups. In addition to the assumption on the conformation of the polyelectrolyte chain, the model proposed can be classified into two groups from the viewpoint of the charge distribution assumed on the polyacid chain: the model with a smeared charge density and the one with a discrete charge distribution. The potentiometric titration of a poly(vinylic carboxylic acid), such as poly(acrylic acid) (PAA), has been successfully analyzed by an infinite rodlike model with the smeared charge density,[1,2] whose surface electrostatic potential, ψ, can be numerically calculated from the direct solution of the Poisson–Boltzmann equation with the aid of a computer.[3,4] It is related to the apparent dissociation constant, $pK_a = pK_0 + 0.4343N_Ae(d\psi/d\alpha)/RT$, as a function of the degree of dissociation, α, where pK_0 is an intrinsic dissociation constant.[5] As the charge density on the polyacid becomes higher, the values calculated from this model would be expected to be in better agreement with the experimental data because the increase in the charge density on a polyacid chain renders the approximation of the smeared charge model more reasonable. In fact Nagasawa et al.[1] reported that the data on the potentiometric titration of PAA at higher α are in better agreement with the calculation than those at lower α. In addition, judging from the chain stiffness of polycrotonate[6-9] or polyfumarate,[10] polymers prepared from monomers having two substituents at both ends of the double bond including poly(fumaric acid) (PFA) and poly(maleic acid) (PMA), both of which have the same molecular formula –(CH(COOH)CH(COOH))–, must have stiffer backbones than PAA. Therefore, the rod model with the smeared charge density should appear to be more suitable for these polyacids.

* Author to whom correspondence should be addressed.
† Present address: Research Center, Polyplastics Co., 973 Miyajima, Fuji 416, Japan.

0024-9297/90/2223-0731$02.50/0

In the previous paper[5] we reported that PFA and PMA appear to dissociate in two steps due to the strong short-range electrostatic interaction from the neighboring ionized groups and that PMA shows a clearer two-step dissociation than PFA possibly due to the configurational difference between them. Moreover, contrary to the above expectation, it was found that the values calculated from the rod model with the smeared charge density, applicable to the dissociation of PAA, could not interpret the electrostatic free energy of both polyacids even in the region of $\alpha < 0.5$ where the overall charge density is equivalent to that of PAA. It is unreasonable for such a simple model to expect the apparent two-step dissociation of PFA and PMA, which should be ascribed to strong short-range interaction between a proton and the neighbors as is the case for the alternating copolymers of maleic acid.[11,12]

An alternative way to evaluate the electrostatic interaction during dissociation is a direct summation of the Coulombic interactions between all pairs of the charges as proposed by Tanford.[13,14] This procedure could in principle be applicable to any polyelectrolyte but is still limited to a very simple case, although this method will be tried in the future when a more powerful computer is available. Recently a discrete-site model for hyaluronic acid with very low charge density was proposed by Cleland[15] who calculated its pK_a by averaging over the possible conformations of the chain with discrete charges.

There have been several studies concerning the statistical thermodynamics of the discrete-site model.[16-20] We proposed an improved method[12] which is useful for the interpretation of titration of the alternating copolymer of maleic acid with isobutylene if we take into account either that the local dielectric constant is lower than its bulk value or that hydrogen bonding occurs between the neighboring carboxyl groups. One of the characteristics of our method is that we explicitly divide the electrostatic interaction between a proton and the ionized groups into short-range and long-range interactions and that we evaluate each interaction separately in contrast to the models assuming a uniform charge density. Norisuye et al.[21] also reported that a similar model can better account for the dissociation behavior of rigid double-helical xanthan with a low charge density than can the cylinder model uniformly charged, where they cut off the long-range electrostatic interaction at an arbitary distance in order to fit the calculated values to the observed ones. Merle[22] applied this method to the potentiometric titration curve of polyampholytes, taking into account only the nearest-neighbor interactions of charges with opposite signs and neglecting the long-range interaction.

The present paper is aimed at deriving the expression for the potentiometric titration of both polyacids by using the Ising model with short-range interaction in the same way as reported previously.[11,12,20] Possible configurations of PFA and PMA are assumed. The factors considered in the model calculation to compare with the experimental result include: the range of the short-range interaction, the configuration of the carboxyl groups, the value of the dielectric constant around the ionized groups, and the hydrogen bond between the carboxyl groups in the neighbors.[12,23] In addition to the short-range interaction, we will discuss the natures of the long-range electrostatic interaction characteristic of the polyacids with higher charge densities.

Model Calculation

1. General Expression. Throughout this paper we are concerned only with the electrostatic part of pK_a, which is represented by ΔpK. If pK_0 is independent of α, then

$$\Delta pK = pK_a - pK_0 \tag{1}$$

which is further divided into two terms

$$\Delta pK = \Delta pK_{short} + \Delta pK_{long} \tag{2}$$

where ΔpK_{short} is the term due to the short-range interaction, and ΔpK_{long}, the term due to the long-range interaction not counted in ΔpK_{short}. In general, ΔpK_{short} is expressed as follows:[11,12,18]

$$\Delta pK_{short} = \log a + \log [(1 - \alpha)/\alpha] \tag{3}$$

$$a = a_-/a_0 \tag{4}$$

where a_- and a_0 are the activities of the dissociated $-COO^-$ and the undissociated $-COOH$ groups, respectively. Therefore, using the common procedures of statistical mechanics, α is derived from the grand partition function, Ξ, of a polyacid as a function of the activity ratio a. As for the diprotic polyacids such as PFA and PMA with the degree of polymerization N, Ξ is[11,12]

$$\Xi = \sum_{0,-} \prod_{i=1}^{N-1} [a_{2i-1} \exp(-E_{2i-1}/kT) a_{2i} \times \exp(-E_{2i}/kT)] a_{2N-1} \exp(-E_{2N-1}/kT) a_{2N} \tag{5}$$

where the summation is carried out over the possible combination of states for all dissociation groups, with a_j equal to either a_0 or a_- corresponding to the unionized or the ionized states, respectively, E_j, the energy of the interaction governing the dissociation state of the jth dissociation group, k, the Boltzmann constant, and T, the absolute temperature. We will estimate E_j by the pairwise Coulombic potential at a short distance, which depends on the specific configuration of the $-COOH$ group. Then α will be calculated effectively by means of the transition matrix whose elements correspond to the relative probability of the state correlated to E_j, since, as will be shown later, α is related to a through Ξ.

The term ΔpK_{long} due to the long-range interaction from the dissociation groups other than those counted in the short-range interaction is assumed to be represented by the Debye–Hückel potential. Namely, ΔpK_{long} can be calculated by summation of the potentials as

$$\Delta pK_{long} = 0.4343\alpha/kT \sum_{P_i=P_s+1}^{2N} (e^2/DR_{P_i}) \exp(-\kappa R_{P_i}) \tag{6}$$

where κ is the Debye–Hückel parameter and the summation is carried out over the pairs of the interaction not included in the short-range interaction in eq 5. For example, in the case of the second nearest-neighbor short-range interaction, the summation starts from the interaction between the $(2i - 1)$th and the $(2i + 2)$th groups and then that between the $2i$th and the $(2i + 3)$th and is repeated until it does not increase by more than 0.5% on adding the next term. The number of terms in the summation of eq 6 is usually below 20 at $C_s = 0.10$ N NaCl. Strictly speaking, it is necessary to average the calculation of ΔpK_{long} over the possible conformational distribution of dissociating groups. Such averaging is rather difficult, however, since the conformational properties of the polyelectrolyte chain including the electrostatic excluded-volume effect have not yet been elucidated completely,[24] although now we are on the way to a reasonable understanding of it.[25] The model calculation without averaging for the fixed typical conformations seems to be sufficient to describe the dissociation behavior characteristic of PMA and PFA.

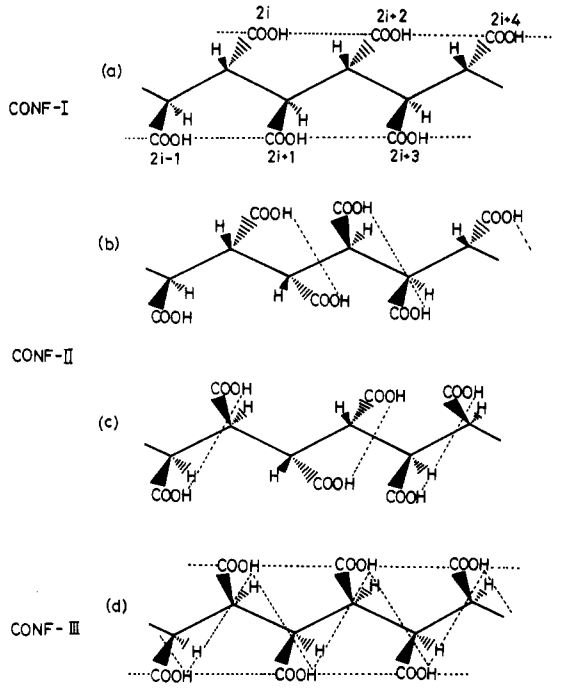

Figure 1. Possible configurations of –COOH for PFA and PMA, assuming a main chain as an extended trans zigzag conformation: (a) erythro diisotactic ($g^+g^+g^+g^+$) as CONF-I; (b) disyndiotactic ($g^+g^+g^-g^-$) as CONF-II; (c) disyndiotactic ($g^+g^-g^-g^+$), the same configuration as (b); (d) threo diisotactic ($g^+g^-g^+g^-$) as CONF-III. The dotted lines represent possible formation of hydrogen bondings between neighbors.

2. Molecular Configuration. The starting materials of PFA and PMA were bis(trimethylsilyl)fumarate in the trans configuration and maleic anhydride in the cis configuration, respectively.[5,10] Therefore, PMA and PFA may have a complicated configuration called ditacticity,[26] which depends on the orientations of the two –COOH groups originally situated at both ends of the double bond in the monomer. As discussed by Barone et al.,[27] these groups could dissociate in more than two steps. We also reported previously[5,10] that, from the viewpoint of the preparation methods of PMA and PFA, there should be some difference in the configurations between both polyacids, which have not yet been determined by such spectroscopic methods as NMR or IR. Probably any two successive diads in such a chain are formed through two different mechanisms with different tactic probabilities, where the probability for one of the two diads is related to the addition mode and the other is related to chain-end rotation, so that the propagation step in α,β-disubstituted monomers generates two pseudoasymmetric centers. As for the polyfumarates, a few reports have been published recently that the extent of meso and racemic diads for poly(diisopropyl fumarate) are 0.78 and 0.22, respectively, by ^{13}C NMR[28] and by X-ray diffraction analysis in the crystalline state.[29] It is also well-known that dialkyl fumarates can polymerize by free-radical polymerization, but the cis isomers, dialkyl maleates, can polymerize only with difficulty. This fact clearly suggests that the rate of rotation around the C–C backbone in the chain end is much slower than that of propagation. Accordingly, it seems reasonable to assume that both polyacids retain their monomer configurations. We selected the configurations shown in Figure 1 as the typical ones for both polyacids. The main chain of each polyacid is assumed to have an extended trans planar zigzag conformation, probably because of electrostatic repulsion between the ionized groups on the chain, and to retain this conformation during neutralization, as confirmed by Muroga et al.[30,31]

Let a particular –COOH group, for example, the $(2i - 1)$th from the chain end, be assigned a gauche$^+$ conformation, g^+, with respect to the main chain. For a PFA chain, two –COOH groups, the $(2i - 1)$th and the $2i$th, assumed to belong originally to the same monomer, may remain in the opposite direction so that they have the same g^+ conformation with respect to the main chain, assumed to be trans. In the polymerization process of di-*tert*-butyl fumarate, the succeeding monomer may prefer to link to the preceding from the opposite side due to the bulky $2i$th *tert*-butyl ester group at the polymerization end; that is, the conformation of the $(2i + 1)$th is likely to have a g^+ conformation with respect to the main chain and consequently the $(2i + 2)$th has a g^+ conformation. The most probable configuration of PFA is, therefore, the one shown in Figure 1a, which is called erythro diisotactic.[26] Another one, called disyndiotactic,[26] is shown in Figure 1b, although it seems more unlikely than the former because of the large steric hindrance of substituents. In fact, the most probable configuration of poly(dialkyl fumarate), proposed by Ando et al.,[28] is the one shown in Figure 1a rather than in Figure 1b.

On the other hand, for PMA the $(2i - 1)$th and the $2i$th groups, originally from the same monomer, are presumed not to move far apart from each other after hydrolysis in order to preserve the configuration of the starting monomer, maleic anhydride. Thus, if the conformation of the $(2i - 1)$th is assigned to g^+ with respect to the main chain, then it seems natural for the $2i$th to have a g^- conformation, where the $2i$th remains rather close to the $(2i - 1)$th. In the polymerization of maleic anhydride, there are still two possible directions for the next monomer to link to the preceding monomer, in the same way as those for PFA, as shown in parts c and d of Figure 1. The configuration in Figure 1c is essentially the same disyndiotactic as in Figure 1b while that in Figure 1d is called threo diisotactic.[26]

Although actual configurations are not as completely regular as those in Figure 1, the model calculation for the potentiometric titration of PFA and PMA was carried out only for these three configurations as the typical configurations for PFA and PMA, which are shown in Figure 1a denoted as CONF-I, Figure 1b,c as CONF-II, and Figure 1d as CONF-III.

The molecular parameters for determining the distance between the dissociating groups for each configuration were presented in the previous paper.[12] A proton and a charge of the carboxyl groups are assumed to be situated at the center between the two oxygens in the carboxylate ion, $-COO^-$. Along the main chain from the $(2i - 1)$th or from the $2i$th groups to their succeeding groups, we assign their neighbors to the first, second, third, and fourth nearest neighbors, respectively, in each configuration. The distances to the nearest neighbors are given in Table I, which shows that the order in the distance is not always in the same order of the sequential number along a chain but depends on the particular configuration considered.

3. Short-Range Electrostatic Interaction. (a) First Nearest-Neighbor Interaction ($P_s = 1$). To begin with, the one-dimensional Ising model with the first nearest-neighbor interaction is applied to the calculation just in the same way as in the previous papers,[11,12] using a matrix method. If we define the matrixes describing the states correlating to the $(2i - 1)$th and the $2i$th dissociation groups

Table I
Distance from (2i - 1)th or 2ith -COOH to Nearest Neighbor -COOH's along the Main Chain

		distance, nm			
config	-COOH	1st	2nd	3rd	4th
CONF-I	2i - 1	0.488	0.252	0.604	0.504
	2i	0.488	0.252	0.604	0.504
CONF-II	2i - 1	0.351	0.421	0.604	0.504
	2i	0.488	0.421	0.500	0.504
CONF-III	2i - 1	0.351	0.252	0.500	0.504
	2i	0.351	0.252	0.500	0.504

as **M** and **M**′, respectively, then Ξ in this system is expressed as

$$\Xi = a_0^{2N}\mathbf{E}(\mathbf{MM}')^{N-1}\mathbf{MA} \tag{7}$$

where the matrixes **E**, **A**, **M**, and **M**′ are as follows:

$$\mathbf{E} = (1 \quad 1) \qquad \mathbf{A} = (1 \quad a)^{\mathrm{T}} \tag{8}$$

$$\mathbf{M} = \mathbf{M}(u) = \begin{bmatrix} 1 & 1 \\ a & ua \end{bmatrix} \qquad \mathbf{M}' = \mathbf{M}(u') \tag{9}$$

The superscript T indicates a transposed matrix. The parameters denoted by u and u' are the statistical weights of the states of the (2i - 1)th and 2ith groups, respectively, on the basis of the statistical weight of the unionized state as 1. For Coulombic potential, they are expressed as

$$u = u(R_1) = \exp(-e^2/DkTR_1) \qquad u' = u(R_1') \tag{10}$$

where D is the dielectric constant in the medium between the interacting groups, and R_1 and R_1' are the distance from (2i - 1)th to the 2ith and that from 2ith to the (2i + 1)th, respectively. It is not clear whether the value of D is actually the same as that in the bulk or not. We will discuss later the effect of the value of D upon the calculated ΔpK.

If the largest eigenvalue, λ_1, of the matrix product **MM**′ is determined, α can be obtained by[11,12,18]

$$\alpha = (1/2)\,(\mathrm{d}\log\lambda_1/\mathrm{d}\log a) \tag{11}$$

since Ξ is approximately equal to λ_1^{N-1} for sufficiently large N. For convenience in the higher dimensional matrixes used later, λ_1 is determined here not analytically by solving the characteristic equation but numerically by a computer using a so-called power method. The numerical value of λ_1 thus determined was confirmed to be equal to the analytical one within an error of 10^{-8}. Using eq 11, the value of α can be deduced for a given a by taking the ratio of the increment of λ_1 to the relative increase in a by 10^{-4}% for the specified configuration in Figure 1, that is, for the specific values of u and u'. Thus we can evaluate $\Delta pK_{\mathrm{short}}$ for the specific configuration by substituting the value of a and α thus determined in eq 3.

(b) Second to the Fourth Nearest-Neighbor Interaction (P_s = 2–4). In the same way as described above, the matrixes in eq 8 and 9 including up to the second to the fourth nearest-neighbor interaction are derived by introducing the parameters v and v' for the second, s and s' for the third, and w and w' for the fourth nearest-neighbor interactions. The parameters v and v' are defined in the same way as in eq 10

$$v = u(R_2) \qquad v' = u(R_2') \tag{12}$$

where R_2 and R_2' are the distance from the (2i - 1)th to the (2i + 1)th and that from the 2ith to the (2i + 2)th groups, respectively. The other parameters are defined in the same way. The form of the matrixes for the second nearest-neighbor interaction has already been written in the previous paper.[12]

For the third nearest-neighbor interaction the expressions of the matrixes are given by introducing the following two submatrixes $\mathbf{P}(s,u)$ and $\mathbf{Q}(s,u)$.

$$\mathbf{P}(s,u) = \begin{bmatrix} 1 & s & 0 & 0 \\ 0 & 0 & u & us \\ 0 & 0 & 0 & 0 \\ 0 & 0 & 0 & 0 \end{bmatrix}$$

$$\mathbf{Q}(s,u) = \begin{bmatrix} 0 & 0 & 0 & 0 \\ 0 & 0 & 0 & 0 \\ 1 & s & 0 & 0 \\ 0 & 0 & u & us \end{bmatrix} \tag{13}$$

Namely

$$\mathbf{E} = (1 \quad 1 \quad 1 \quad 1 \quad 1 \quad 1 \quad 1 \quad 1)$$
$$\mathbf{A} = (1 \quad 1 \quad 1 \quad 1 \quad a \quad a \quad a \quad a)^{\mathrm{T}} \tag{14}$$

$$\mathbf{M} = \mathbf{M}(u,v,s) = \begin{bmatrix} \mathbf{P}(1,1) & \mathbf{Q}(1,1) \\ a\mathbf{P}(s,u) & va\mathbf{Q}(s,u) \end{bmatrix}$$
$$\mathbf{M}' = \mathbf{M}(u',v',s') \tag{15}$$

For the fourth nearest-neighbor interaction the corresponding matrixes are

$$\mathbf{E} = (1 \quad 1 \quad 1 \quad 1 \quad 1 \quad 1 \quad 1 \quad 1 \quad 1 \quad 1 \quad 1 \quad 1 \quad 1 \quad 1 \quad 1 \quad 1)$$
$$\mathbf{A} = (1 \quad 1 \quad 1 \quad 1 \quad 1 \quad 1 \quad 1 \quad 1 \quad a \quad a \quad a \quad a \quad a \quad a \quad a \quad a)^{\mathrm{T}} \tag{16}$$

$$\mathbf{M} = \mathbf{M}(u,v,s,w) = \begin{bmatrix} \mathbf{P}(1,1) & \mathbf{Q}(1,1) & \mathbf{0} & \mathbf{0} \\ \mathbf{0} & \mathbf{0} & \mathbf{P}(1,1) & \mathbf{Q}(1,1) \\ a\mathbf{P}(w,s) & va\mathbf{Q}(w,s) & \mathbf{0} & \mathbf{0} \\ \mathbf{0} & \mathbf{0} & ua\mathbf{P}(w,s) & uva\mathbf{Q}(w,s) \end{bmatrix}$$
$$\mathbf{M}' = \mathbf{M}(u',v',s',w') \tag{17}$$

where **0** is the 4 × 4 zero matrix.

4. Hydrogen Bonding. Since the carboxylic acid groups of PFA and PMA exist close to each other, the formation of the intramolecular hydrogen bonding between them should be considered. In fact we confirmed the existence of hydrogen bonding in PMA in infrared spectroscopic measurements.[23] The hydrogen bonding is one of the short-range interaction so that its effect should be added to the term $\log a$. In contrast to electrostatic interaction, however, it is a specific or a cooperative interaction which depends strongly on the configuration of -COOH. Therefore, we must examine the effect of hydrogen bonding individually for each configuration shown in Figure 1, where the possible pairs of hydrogen bonding are denoted by dotted lines. Taking into account the fact that the alternating copolymer of maleic acid has also intramolecular hydrogen bonding in an aqueous solution[23] while PAA has no evidence on the formation of hydrogen bonding,[32] we assume here that all pairs of the carboxyl groups separated at the distance less than 0.4 nm may form the hydrogen bond. Judging from the cooperative natures of hydrogen bonding, a -COOH group cannot form hydrogen bondings of more than two. In contrast to CONF-II where a pair of hydrogen bondings is definite as shown, there are two choices in CONF-I for the (2i + 1)th to form hydrogen bonding, either to the (2i - 1)th or to the (2i + 3)th with equal probability, and there are even four choices of hydrogen bonding in CONF-III where the energy of hydrogen bonding may depend on the distance of the pair.[33,34] For simplicity, however, we assume here that the effect of hydrogen bonding is

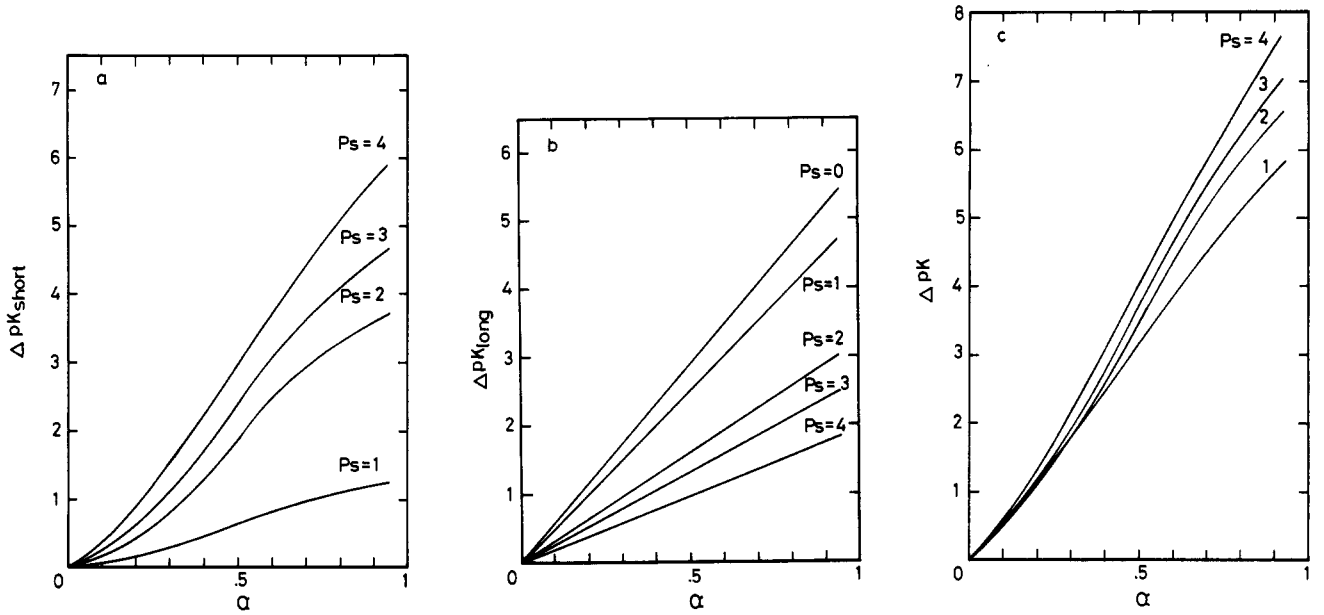

Figure 2. Dependence of the electrostatic interaction on the range of the short-range interaction adopted, P_s, for CONF-I: (a) ΔpK_{short}, (b) ΔpK_{long}, and (c) ΔpK.

taken into account just within the range corresponding to the short-range interaction.

For the first nearest-neighbor interaction, **M** and **M′** can be rewritten in the following manner for CONF-II. The multiselection of hydrogen bondings for the other configurations leads to rather complicated calculations, where **M** and **M′** have 36 × 36 dimensions for CONF-I and even 100 × 100 for CONF-III, respectively. Therefore, the effect of hydrogen bonding on the dissociation behavior will be discussed here only for CONF-II. The matrixes **M** and **M′** in eq 9 are replaced as

$$\mathbf{M} = \begin{bmatrix} h_0 & 0 & h_- & 0 \\ 0 & 1 & 0 & 1 \\ h_-a & 0 & 0 & 0 \\ 0 & a & 0 & ua \end{bmatrix}$$

$$\mathbf{M}' = \begin{bmatrix} 1 & 1 & 1 & 1 \\ 1 & 1 & 1 & 1 \\ a & a & u'a & u'a \\ a & a & u'a & u'a \end{bmatrix} \qquad (18)$$

For the second nearest-neighbor interaction, **M** and **M′** have already been expressed.[12] The statistical weights due to the hydrogen bonding, h_0 and h_- are defined by

$$h_0 = h(H_0) = \exp(-H_0/kT) \qquad h_- = h(H_-) \qquad (19)$$

where H_0 and H_- are the apparent energies of the hydrogen bondings between -COOH and -COOH and between $-COO^-$ and -COOH, respectively. Actually, however, we will not distinguish between them and will use H as the average for them.

Results

We examined first the results of the model calculation for CONF-I in detail to clarify the factors affecting the electrostatic interaction. Figure 2 shows the values of ΔpK as well as ΔpK_{short} and ΔpK_{long} for the various ranges of the short-range interaction, P_s, where the concentration of added salt, C_s = 0.10 N, T = 298 K, and D = 78. When P_s, defined as the range of short-range interaction, is expanded from 1 to 4, ΔpK_{short} increases while ΔpK_{long} decreases, so that ΔpK, represented by the sum of both, increases rather slightly as a result. The tendency of ΔpK was similar for the other configurations. An inflection point at α = 0.5, characteristic of ΔpK_{short}, becomes less clear on increasing P_s. The term of ΔpK_{long} proportional to α makes such an inflection point unclear. It is concluded from Figure 2 that the apparent two-step dissociation characteristic of PFA and PMA should be ascribed to the contribution of the short-range interaction as expected from the previous results.[11,12]

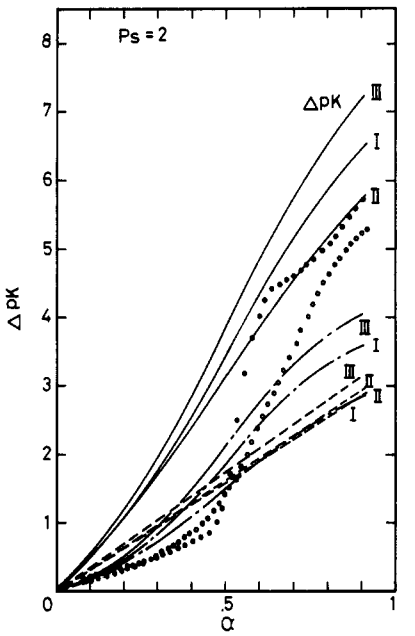

Figure 3. Effect of the configuration on the electrostatic interaction for P_s = 2. Solid, chain, and broken lines represent the ΔpK, ΔpK_{short}, and ΔpK_{long}, respectively. The open and filled circles are experimental data for PFA and PMA, respectively, in ref 5.

For comparison, the results of the model calculation for the other configurations under the same conditions as in Figure 2 are presented in Figure 3 for P_s = 2. The dependence of ΔpK on the configuration seems to support the assumption in the previous paper[5] that the difference in the titration behavior between PFA and PMA is ascribed to their configurational difference. Among the configurations examined here the configuration III shows the clearest inflection point whereas the configu-

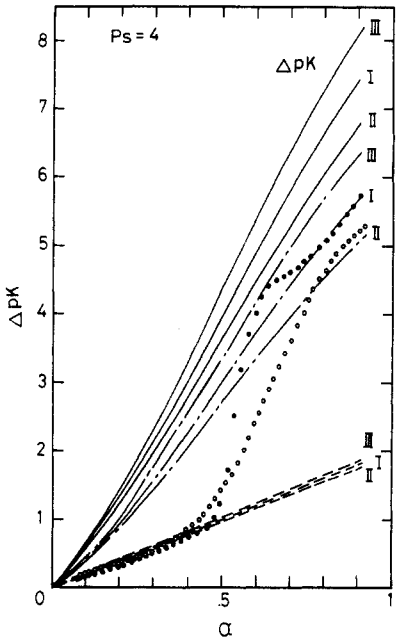

Figure 4. Effect of the value of dielectric constant, D, on ΔpK at $P_s = 2$ for CONF-I. Solid and chain lines represent ΔpK and ΔpK_{short}, for $D = 78$, 30, and 22, from bottom to top, respectively. The circles are the same as in Figure 3.

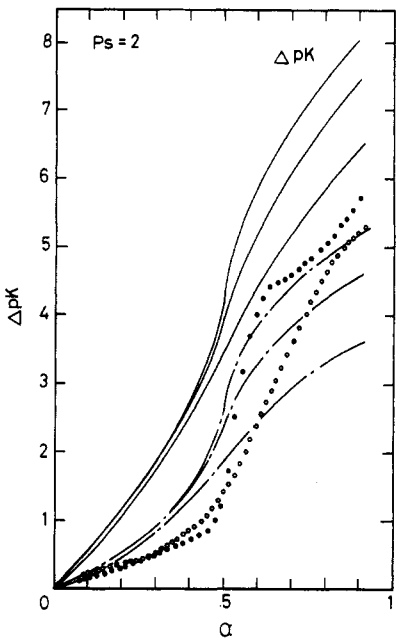

Figure 5. Effect of the energies of the hydrogen bonding, H, on ΔpK at $P_s = 2$ for CONF-II. Solid and chain lines represent ΔpK and ΔpK_{short} for $H = 0$, −6.7, −11.7, and −16.0 kJ mol^{-1}, from bottom to top, respectively. The circles are the same as in Figure 3.

ration II has the least clear one. The clear appearance of an inflection point in ΔpK_{short} is also related to the range in the short-range interaction, P_s, and the ratio of R_i to R_i'. That is, either with smaller P_s or with larger R_i/R_i', an inflection point becomes clearer. But the experimental data of the titration of PFA and PMA, denoted by circles on the same figures, do not agree quantitatively with the results of model calculation but for the qualitative tendencies. The disagreements of the calculation with the experiments were found in the absolute value of ΔpK itself and in the extent of the jump around $\alpha = 0.5$.

To improve the agreement, the effect of the dielectric constant D around the ionized groups on ΔpK was introduced in the same way as in the previous paper.[12] The actual value of D in the molecular dimension has not been known but is expected reasonably to be rather smaller than its bulk value, 78,[19] and to vary with the distance between ionized groups.[35] The effect of the value of D involved in the short-range interaction in eq 10 and 12 on the calculation is shown in Figure 4 for CONF-I with the second nearest-neighbor interaction as the short-range interaction while D in the long-range interaction in eq 6 remains 78. This figure indicates that the decrease of D in the short-range interaction results in the clearer inflection point and in the increase in the magnitude in ΔpK at α higher than 0.5. Therefore, the introduction of the smaller value of D to the model calculation seems to improve the agreement with the experimental results in the more definite appearance of an inflection point in ΔpK. However, the magnitude of ΔpK becomes much larger than the experimental value.

The results of the model calculation for CONF-II with the second nearest-neighbor short-range interaction in the presence of the hydrogen bonding are shown in Figure 5 where ΔpK is plotted for the different values of the energy of the hydrogen bonding, H. It is found in this figure that as the value of H becomes larger the jump in ΔpK at $\alpha = 0.5$ becomes more distinct and the absolute value of ΔpK becomes larger, in a way similar to the effect of dielectric constant introduced in Figure 4. However, the quantitative agreement of the calculation with the experiments is still unsatisfactory.

Discussion

Among the electrical properties of the polyelectrolyte solution in the presence of salt, the potentiometric titration is closely related to the electrostatic interaction between a proton and ionized groups on a polyion. Although the electrostatic interaction can be transmitted to a longer distance in such a functional form as the direct Coulombic or the Debye–Hückel potential, it is the electrostatic short-range interaction that has a primary effect on the dissociation behavior of polyacids.

As shown in Figure 2, the inflection point at $\alpha = 0.5$ characteristic of the titration curves of PFA and PMA becomes less clear with the expansion of the order of the short-range interaction from $P_s = 1$ to 4. That is, the apparent two-step dissociation of PFA and PMA results from the short-range interaction, especially, the first and second ones. The conclusion reached here is the same as in the previous papers for the maleic acid copolymers.[11,12]

The dependence of the configuration on the model calculation of ΔpK_{short}, shown in Figure 3, leads to another conclusion: that the configurations are different between PFA and PMA, which is obtained from the comparison with the titration data.[5]

We reported previously that the model calculation is even quantitatively in better agreement with the experiments for the alternating copolymer of maleic acid if either the lower dielectric constant near the ionized groups or the formation of hydrogen bonding between the nearest-neighbor groups is introduced.[12] In the present study, however, the effect of dielectric constant and hydrogen bonding did not provide as good quantitative agreement with the experimental data as shown in Figures 4 and 5. When these results are examined in detail, the poorer agreement in the present model calculation even including such effects appears to come mainly from the overestimation of ΔpK_{long} term where the electrostatic

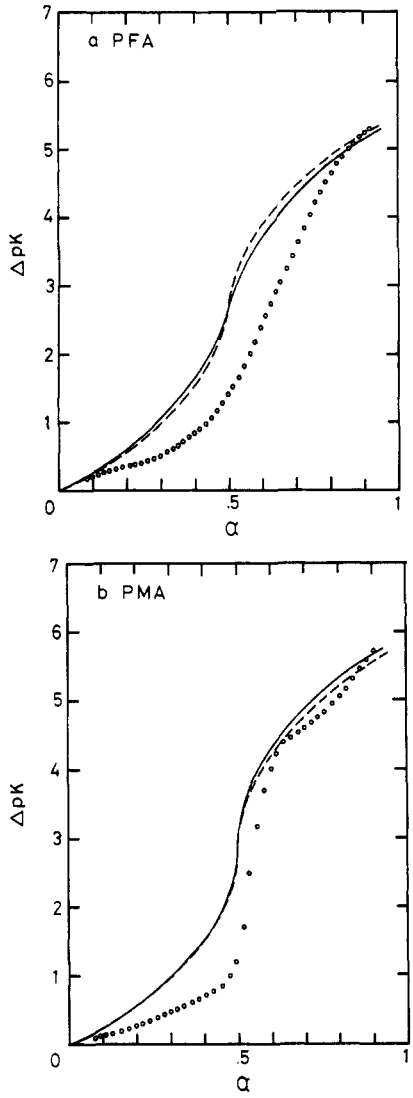

Figure 6. Comparison of the model calculation for $P_s = 2$ with the experimental data[5] denoted by circles: (a) PFA; solid line, $D = 28$ for CONF-I; broken line, $H = -10.7$ kJ mol^{-1} for CONF-II, at $C_s^* = 1.0$ N. (b) PMA; solid line, $D = 30$ for CONF-II; broken line, $H = -12.4$ kJ mol^{-1} for CONF-II, at $C_s^* = 1.0$ N.

interaction is assumed as Debye–Hückel potential. There is a great difference in the estimation of ΔpK_{long} between the present study on PFA or PMA and the previous one on the copolymer of maleic acid; that is, PFA and PMA have charge densities twice as high as in the previous one.[12] To reduce the value of ΔpK_{long} in the model calculation, one might cut off the summation in eq 6 at an arbitrary term.[21,22] However, we select here another way of correction to reduce ΔpK_{long} since the cutoff of the long-range interaction seems quite arbitrary. We also reported previously that, at higher α than 0.5, the intrinsic viscosities of PFA and PMA decrease with increasing α until the solutions become turbid.[5] This is due to what we called "local salting out" at higher α, since the extent of turbidity increases with increasing concentration of added salt. That is, it is ascribed to the local salt concentration, C_s^*, being higher than bulk. We assumed C_s^* to remain as constant. In Figure 6, ΔpK is calculated both from ΔpK_{short} including the effect of D or H and from ΔpK_{long} with $C_s^* = 1.0$ N compared to that in bulk, 0.10 N. The values of D were assumed tentatively but closely agreed with the values calculated from the theory of Kirkwood and Westheimer.[36] These figures, especially for PMA, show rather satisfactory agreement of the model calculation with the experimental data. Therefore, it is necessary to adopt a local salt concentration larger than the bulk in order to fit the calculation to the experimental data for PFA and PMA because of their higher charge densities. The assumption of local salt concentration may provide the same effect as the cutoff of the contribution from the longer electrostatic interaction[21,22] or the ion condensation proposed by Manning.[37] The local salt concentration may not be a constant but increases with α leading to the decrease in ΔpK_{long}. In the region of high α, however, the effective dielectric constant of the medium in the vicinity of an ionized group becomes lower, resulting in the increase in ΔpK_{long}. The latter effect seems to compensate that of the former at least qualitatively, which supports the tentative assumption of an apparently constant value of C_s^* during neutralization.

To improve the model calculation, we cannot avoid the asymmetric natures of the titration data for both polyacids where the experimental curves show lower increase in ΔpK for $\alpha < 0.5$ and higher increase for $\alpha > 0.5$. It is rather difficult to deduce such behavior from the model calculation. Since the Ising model itself is symmetric, we must introduce the asymmetric natures into ΔpK_{long}. We will have to discuss the problem further in the future.

Registry No. PFA, 9003-16-1; PMA, 26099-09-2.

References and Notes

(1) Nagasawa, M.; Murase, T.; Kondo, K. *J. Phys. Chem.* **1965**, *69*, 4005.
(2) Kawaguchi, Y.; Nagasawa, M. *J. Phys. Chem.* **1969**, *73*, 4382.
(3) Kotin, L.; Nagasawa, M. *J. Chem. Phys.* **1962**, *36*, 873.
(4) Sugai, S.; Nitta, K. *Biopolymers* **1973**, *12*, 1363.
(5) Kitano, T.; Kawaguchi, S.; Ito, K.; Minakata, A. *Macromolecules* **1987**, *20*, 1598.
(6) Kitano, T.; Fujimoto, T.; Nagasawa, M. *Macromolecules* **1974**, *7*, 719.
(7) Noda, I.; Imai, T.; Kitano, T.; Nagasawa, M. *Macromolecules* **1981**, *14*, 1303.
(8) Noda, I.; Imai, T.; Kitano, T.; Nagasawa, M. *Macromolecules* **1981**, *14*, 1306.
(9) Muroga, Y.; Sakuragi, I.; Noda, I.; Nagasawa, M. *Macromolecules* **1984**, *17*, 1844.
(10) Kitano, T.; Ishigaki, A.; Uematsu, G.; Kawaguchi, S.; Ito, K. *J. Polym. Sci., Polym. Chem. Ed.* **1987**, *25*, 979.
(11) Minakata, A.; Matsumura, K.; Sasaki, S.; Ohnuma, H. *Macromolecules* **1980**, *13*, 1549.
(12) Kitano, T.; Kawaguchi, S.; Anazawa, N.; Minakata, A. *Macromolecules* **1987**, *20*, 2498.
(13) Tanford, C.; Kirkwood, J. G. *J. Am. Chem. Soc.* **1957**, *79*, 5333.
(14) Tanford, C. *J. Am. Chem. Soc.* **1957**, *79*, 5340.
(15) Cleland, R. L. *Macromolecules* **1984**, *17*, 634.
(16) Marcus, R. A. *J. Am. Chem. Soc.* **1954**, *58*, 621.
(17) Harris, F. E.; Rice, S. A. *J. Phys. Chem.* **1954**, *58*, 725.
(18) Lifson, S. *J. Chem. Phys.* **1957**, *26*, 727.
(19) Schultz, A. W.; Strauss, U. P. *J. Phys. Chem.* **1972**, *76*, 1767.
(20) Sasaki, S.; Minakata, A. *Biophys. Chem.* **1980**, *11*, 199.
(21) Zhang, L.; Takematsu, T.; Norisuye, T. *Macromolecules* **1987**, *20*, 2882.
(22) Merle, Y. *J. Phys. Chem.* **1987**, *91*, 3092.
(23) In preparation.
(24) Noda, I.; Tsuge, T.; Nagasawa, M. *J. Phys. Chem.* **1970**, *74*, 710.
(25) Inagaki, H.; Yukioka, S.; Hayakawa, M.; Noda, I.; Nagasawa, M.; Kitano, T. *Polym. Prepr. Jpn.* **1985**, *34*, 2701.
(26) Huggins, M. L.; Natta, G.; Desreux, V.; Hark, H. *J. Polym. Sci.* **1962**, *56*, 153.
(27) Barone, G.; Rizzo, E. *Gazz. Chim. Ital.* **1973**, *103*, 401.
(28) Wang, X.; Komoto, T.; Ando, I.; Otsu, T. *Makromol. Chem.* **1988**, *189*, 1845.
(29) Cortizo, M. S.; Macchi, E. D.; Figini, R. V. *Polym. Bull. (Berlin)* **1988**, *19*, 477.
(30) Muroga, Y.; Noda, I.; Nagasawa, M. *Macromolecules* **1985**, *18*, 1576.
(31) Muroga, Y.; Noda, I.; Nagasawa, M. *Macromolecules* **1985**, *18*, 1580.

(32) Leyte, J. C.; Zuiderweg, L. H.; Vledder, H. J. *Spectrochim. Acta* **1967**, *23A*, 1397.
(33) Lippincott, E. R.; Schroeder, R. *J. Chem. Phys.* **1955**, *23*, 1099.
(34) Poland, D.; Scheraga, H. A. *Biochemistry* **1967**, *6*, 3791.
(35) Hopfinger, A. J. *Conformational Properties of Macromolecules*; Academic Press: New York, 1973.
(36) Ninomiya, A.; Toei, K. *Nippon Kagaku Zasshi* **1969**, *90*, 655.
(37) Manning, G. S. *J. Chem. Phys.* **1969**, *51*, 924.

Diffusion of Weakly Confined Star and Linear Polymers and Strongly Confined Linear Polymers in a Porous Material

Nalini Easwar† and Kenneth H. Langley*

Department of Physics and Astronomy, University of Massachusetts, Amherst, Massachusetts 01003

F. E. Karasz

Polymer Science and Engineering Department, University of Massachusetts, Amherst, Massachusetts 01003. *Received January 19, 1989; Revised Manuscript Received May 23, 1989*

ABSTRACT: We report the direct measurement, by dynamic light scattering, of the macroscopic diffusion coefficient D_∞ (at low q) of linear, four-arm star and eight-arm star polyisoprene in silica controlled pore glass, for values of the confinement parameter $\lambda_H = R_H/R_p < 0.1$, where R_H is the hydrodynamic radius of the polymer and R_p is the radius of the pores in the glass. The reduced diffusion in the pores is found to depend on the molecular architecture of the polymer. For a given λ_H, the branched polymers diffuse slower than the linear polymer; it is also found that eight-arm stars diffuse more slowly than four-arm stars of the same hydrodynamic radius. The results are compared to hydrodynamic theories for hard spheres in isolated cylindrical pores. Our results indicate that the hydrodynamic radius of a polymer derived from its diffusion coefficient in dilute unbounded solution does not uniquely describe the hydrodynamic effects of a constraining wall on its diffusion behavior. We also report measurements of the macroscopic diffusion D_∞ of strongly confined linear polystyrene chains with λ_H values up to 0.74. Over the range of confinement investigated, an asymptotic region described by a power law relationship between D_∞ and molecular weight is not observed. Our data suggest that the presence of two length scales in the porous material could play an important role in the diffusion of strongly confined chains, in accordance with the theoretical model of Muthukumar and Baumgartner.

Introduction

The study of polymer transport in porous media has theoretical importance as well as relevance to many phenomena of technological and scientific interest. Experiments such as transport across track-etched membranes,[1-4] transcient diffusion into porous glass,[5,6] and broadening of chromatographic peaks[7] have been directed toward relating macroscopic diffusion to the microscopic parameters characterizing the polymer and the porous medium. The major disadvantage of these phenomenological techniques is that knowledge of the boundary layer resistance to transport and the equilbrium partitioning coefficient of the polymer between the unbounded solution and the pore space are necessary for the interpretation of the data. Attempts to explore directly the movement of molecules *within* the porous medium have employed the experimental techniques of forced Rayleigh scattering,[8] pulsed field-gradient spin-echo NMR,[9] and quasi-elastic light scattering.

Recently, Bishop et al.[10,11] have reported the direct measurement of the diffusion of linear flexible polystyrene in porous glasses by quasi-elastic light scattering (QELS). This technique has the advantage of probing directly the diffusion in pores inside a single fragment of porous material, under thermodynamic equilibrium conditions. These measurements showed that the reduced diffusion in the controlled pore glasses relative to the unbounded solution can be understood in terms of structural effects and hydrodynamic interactions, which are separable phenomena. For small λ_H, the diffusion of these polymers can be considered as the diffusion of equivalent hard spheres. Data for $0 < \lambda_H < 0.23$ fit well to the Brenner and Gaydos theory[12] for the diffusion of hard spheres in isolated cylindrical pores. The plots also yielded values for the intrinsic conductivity X_0 of these glasses. As the ratio of the size of the polymer to that of the pore increased, the hydrodynamics of the confined flexible polymers showed a transition from non-free draining (analogous to hard sphere) to free draining (analogous to Rouse chain) behavior. The maximum confinement parameter reached in these measurements was $\lambda_H = 0.47$.

The research reported in this paper extends the previous work by addressing two aspects of polymer diffusion, namely, the effects of molecular architecture and that of strong confinement on the reduced diffusion in the pores. First, the effect of molecular architecture has been investigated by comparing, in three different porous glasses, the diffusion of star polymers of different arm number but comparable molecular weight. A compari-

† Present Address: Department of Physics, Smith College, Northampton, MA 01063.

0024-9297/90/2223-0738$02.50/0